

See discussions, stats, and author profiles for this publication at: <https://www.researchgate.net/publication/231675865>

# Acrylonitrile-Based Copolymer Membranes Containing Reactive Groups: Surface Modification by the Immobilization of Poly(ethylene glycol) for Improving Antifouling Property and Bioco...

ARTICLE *in* LANGMUIR · OCTOBER 2003

Impact Factor: 4.46 · DOI: 10.1021/la035315h

---

CITATIONS

81

---

READS

119

5 AUTHORS, INCLUDING:



Zhi-Kang Xu

Zhejiang University

249 PUBLICATIONS 6,144 CITATIONS

SEE PROFILE



Xiao-jun Huang

Zhejiang University

60 PUBLICATIONS 1,418 CITATIONS

SEE PROFILE



Peng Ye

Zhejiang Sci-Tech University

21 PUBLICATIONS 718 CITATIONS

SEE PROFILE

# Acrylonitrile-Based Copolymer Membranes Containing Reactive Groups: Surface Modification by the Immobilization of Poly(ethylene glycol) for Improving Antifouling Property and Biocompatibility

Fu-Qiang Nie,<sup>†</sup> Zhi-Kang Xu,<sup>\*,†</sup> Xiao-Jun Huang,<sup>†</sup> Peng Ye,<sup>†</sup> and Jian Wu<sup>\*,‡</sup>

*Institute of Polymer Science, and Department of Chemistry, Zhejiang University, Hangzhou 310027, P. R. China*

*Received July 20, 2003. In Final Form: September 12, 2003*

The antifouling property and biocompatibility of a polyacrylonitrile-based copolymer membrane were improved by the immobilization of poly(ethylene glycol) (PEG) on the membrane surface. The studied membranes were fabricated from poly(acrylonitrile-co-maleic acid), in which the carboxyl groups could be conveniently converted into anhydride and then esterified with poly(ethylene glycol). Chemical and morphological changes on the membrane surface were characterized by Fourier transform infrared spectroscopy (FT-IR), elemental analysis (EA), scanning electron microscopy (SEM), and sessile drop contact angle measurements (CA). It was found that the water contact angle of the membrane was reduced and the biocompatibility corresponding to platelets adhesion and protein adsorption was improved significantly with the immobilization of PEG chains on the membrane surface. Furthermore, the permeation behaviors of the base and modified membranes were investigated by bovine serum albumin (BSA) filtration experiments. Membranes containing hydrophilic carboxyl groups or PEG chains showed higher solution flux, lower BSA adsorption, and better flux recovery after cleaning than those of polyacrylonitrile membranes. Particularly, compared with polyacrylonitrile membranes, the PEG-immobilized membrane showed a 6-fold increase in BSA solution flux, 63% reduction in total fouling, and 67% reduction in BSA adsorption.

## Introduction

Polymer surfaces are the phase boundaries that lie between the bulk and the outer environment.<sup>1</sup> The performance of a polymeric material such as a separation membrane relies highly upon the properties of the boundaries in many applications because the interactions between the material and environments occur chiefly on its surfaces. Membrane surfaces that show minimal protein adsorption are very important in many regions, not only for ultrafiltration and biosensors but also for blood contacting implant devices. Polyacrylonitrile (PAN) and acrylonitrile-based copolymers have been successfully applied as membrane materials in the fields of dialysis, ultrafiltration, enzyme-immobilization, and pervaporation.<sup>2–7</sup> However, the relatively poor hydrophilicity and biocompatibility for this type of membrane limit its further applications in aqueous solution, enzyme-immobilized membrane-bioreactors, and biomedical usage. Increasing the hydrophilicity of the membrane surface can reduce fouling and improve biocompatibility for the membranes.<sup>8–12</sup> Therefore, there are many surface modification

methods that have been reported to make ideal hydrophilic and antifouling surfaces. Among them, the grafting of hydrophilic monomers on the membrane surface shows some promise.<sup>9–12</sup> However, grafting polymerizations induced by radicals, plasma, an electron-beam,  $\gamma$ -irradiation, and ultraviolet irradiation may result in production of a significant amount of homopolymer or cross-linked polymer. The undesired homopolymer wastes expensive starting materials, and cross-linked polymer is detrimental to membrane filtration, since the membrane pores may become blocked. Moreover, the grafting density (number of grafting sites per area) and grafting polymer chain length cannot be determined independently, much less controlled. To increase the hydrophilicity and reduce the fouling of polyacrylonitrile-based membranes, it may also be one effective method to copolymerize acrylonitrile with vinyl monomers containing reactive groups such as maleic anhydride; these anhydride groups can easily undergo an opening reaction with nucleophilic reagents which contain hydroxyl or amine groups. For example, styrene/maleic anhydride copolymers have been reacted with poly(ethylene glycol) (PEG) to synthesize amphiphilic graft copolymers or thermosensitive and pH-sensitive polymers.<sup>13,14</sup>

PEG is well-known for its extraordinary ability to resist protein adsorption because of its hydrophilicity, large excluded volume, and unique coordination with surrounding water molecules in an aqueous medium.<sup>15</sup> Surface-grafted PEG has also rendered ultrafiltration membranes resistant to oil and protein fouling.<sup>16</sup> In our

\* To whom all correspondence should be addressed. Fax: ++ 86 571 87951773. E-mail: xuzk@ipsm.zju.edu.cn.

<sup>†</sup> Institute of Polymer Science.

<sup>‡</sup> Department of Chemistry.

(1) Kato, K.; Uchida, E.; Kang, E. T.; Uyama, Y.; Ikada, Y. *Prog. Polym. Sci.* **2003**, *28*, 209.

(2) Bhat, A. A.; Pangarkar, V. G. *J. Membr. Sci.* **2000**, *167*, 187.

(3) Trotta, F.; Drioli, E.; Baggiani, C.; Lacopo, D. *J. Membr. Sci.* **2002**, *201*, 77.

(4) Broadhead, K. W.; Tresco, P. A. *J. Membr. Sci.* **1998**, *147*, 235.

(5) Godjevargova, T.; Konsulov, V.; Dimov, A.; Vasileva, N. *J. Membr. Sci.* **2000**, *172*, 279.

(6) Hicke, H.-G.; Lehmann, I.; Malsch, G.; Ulbricht, M.; Becker, M. *J. Membr. Sci.* **2002**, *198*, 187.

(7) Musale, D. A.; Kulkarni, S. S. *J. Membr. Sci.* **1997**, *136*, 13.

(8) Zeman, L. J.; Zydney, A. *Microfiltration and Ultrafiltration: Principles and Applications*; Marcel Dekker: New York, 1996.

(9) Pieracci, J.; Crivello, J. V.; Belfort, G. *Chem. Mater.* **2002**, *14*, 256.

(10) Pieracci, J.; Crivello, J. V.; Belfort, G. *J. Membr. Sci.* **1999**, *156*, 223.

(11) Ma, H.; Bowman, C. N.; Davis, R. H. *J. Membr. Sci.* **2000**, *173*, 191.

(12) Higuchi, A.; Shirano, K.; Harashima, M.; Yoon, B. O.; Hara, M.; Hattori, M.; Imamura, K. *Biomaterials* **2002**, *23*, 2659.

(13) Yin, X.; Stöver, H. D. H. *Macromolecules* **2002**, *35*, 10178.

(14) Hou, S.-S.; Kou, P.-L. *Polymer* **2001**, *42*, 2387.

(15) Jo, S.; Park, K. *Biomaterials* **2000**, *21*, 605.

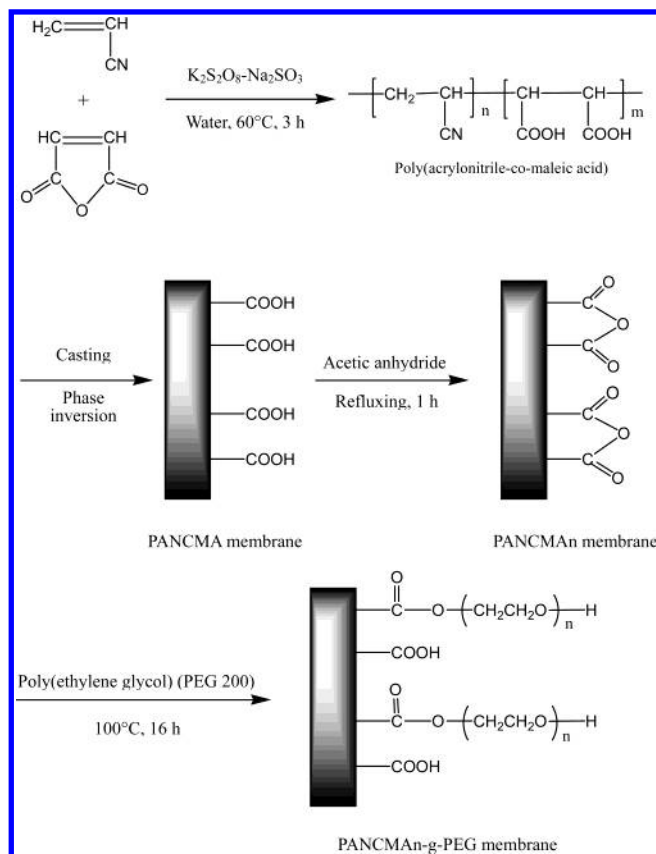


**Figure 1.** Fabrication process for the PAN-based membranes studied in this work.

previous work,<sup>17,18</sup> some efforts have been made to improve the hydrophilicity of polyacrylonitrile-based membranes. Acrylonitrile/maleic acid copolymers were first synthesized by water-phase precipitation copolymerization, which has many advantages such as high molecular weight, relatively high monomer conversion, and environmental friendship compared with common solution copolymerization.

The objective of the present study is to fabricate PAN-based membranes with antifouling properties and good blood compatibility. To achieve this objective, as can be seen from Figure 1, the carboxyl groups on the membrane surfaces of poly(acrylonitrile-co-maleic acid) (PANCMA) were converted into anhydride groups by refluxing the membranes in acetic anhydride, and then these anhydride groups undergo an esterification reaction with PEG containing hydroxyl end groups. After the immobilization of PEG on the membrane surfaces, the virgin and modified membranes were compared with respect to their hydrophilicity, platelet adhesion, water and protein solution permeation, and flux recovery after BSA solution filtration.

### Experimental Section

**Materials.** All chemicals were analytical grade. The polyacrylonitrile (PAN,  $M_w = 25.6 \times 10^4$  g mol<sup>-1</sup>) and poly(acrylonitrile-co-maleic acid) containing 3.69 mol % of maleic acid (PANCMA,  $M_w = 15.8 \times 10^4$  g mol<sup>-1</sup>) were synthesized in our laboratory.<sup>17</sup> Dimethyl sulfoxide (DMSO) was purified by vacuum distillation before used. Bovine serum albumin (BSA, purity > 98%) was purchased from Sino-American Biotechnology

Co. and used as received. A total of 0.1 wt % BSA solution was prepared in a phosphate buffered saline (PBS) solution at pH 7.4. Poly(ethylene glycol) (PEG,  $M_w = 200$  g mol<sup>-1</sup>) was purchased and used without further purification. The nonsolvent coagulation bath selected for the fabrication of flat membranes was ultrafiltrated water, while deionized water was used for the filtration experiment.

**Preparation of Membranes.** PAN and PANCMA were used as membrane materials. Those polymers were dried for at least 3 h at  $60^\circ C$  in a vacuum oven and then dissolved in DMSO at about  $80^\circ C$  for 24 h with vigorous stirring to form a homogeneous 4 wt % casting solution. After air bubbles were removed, the casting solution was cast on a clean glass plate using a casting knife with a  $100\text{ }\mu\text{m}$  gate opening. To fabricate porous membranes, the nascent membranes were placed in the air ( $22 \pm 0.5^\circ C$ , 65–70% relative humidity) for 5 min and then immersed in  $22 \pm 0.5^\circ C$  ultrafiltrated water for 24 h. Then, the membranes were preserved in a 5 vol % formaldehyde solution for further use. These porous membranes were used for the conversion ratio determination of carboxyl to anhydride, element analysis, water adsorption measurement, morphology observation, and filtration experiments. On the other hand, the nascent membranes were dried in an oven at  $120^\circ C$  for 3 h to obtain dense membranes for the water contact angle measurement and platelet adhesion experiment.

**Conversion of Carboxyl Group into Anhydride Group.** The flat membrane of PANCMA was first washed with a water–ethanol–hexane sequence and dried at room temperature. To transfer the reactive group on the membrane surface from carboxyl to anhydride, the dry flat membrane was refluxed in acetic anhydride for 1 h to ensure high conversion.<sup>18</sup> Then, the membrane was thoroughly washed with acetone and dried at  $40^\circ C$  in a vacuum oven for 3 h and was marked as the PANCMAN membrane.

**Determination of Carboxyl and Anhydride Groups on Membrane Surface.** The amount of carboxyl groups on the PANCMAN and PANCMAN porous membranes ( $1 \times 2\text{ cm}^2$ ) was determined by the modified rhodamine–carboxyl interaction method.<sup>19,20</sup> Rhodamine 6 Gx (4 mg) was dissolved in phosphate buffered solution (pH 12, 4 mL), and the solution was immediately extracted with  $100\text{ cm}^3$  of toluene with vigorous shaking in a stoppered Erlenmeyer flask. The extract showed a yellow color and was used as the dye reagent for further experiments. Carboxylic compounds and polymers containing carboxyl groups change their color from yellow to pink at very low carboxyl concentrations. The appearance of the pink color was measured in a spectrophotometer at 513 nm using stoppered cells. For the construction of a calibration curve, known concentrations of maleic acid dissolved in the dye reagent were used. Equal volumes of the two membrane solutions in toluene (1.5 mL) and the dye reagent (1.5 mL) were mixed in clean Pyrex test tubes and allowed to stand for 1 h, and then the optical densities were taken. The conversion ratio of carboxyl groups to anhydride groups on the membrane surface was calculated by the concentration change of carboxyl groups from the PANCMA membrane to the PANCMAN membrane.

**Grafting PEG onto the Membrane.** A dry PANCMAN membrane was immersed in PEG at  $100^\circ C$  under a nitrogen atmosphere for about 16 h.<sup>21,22</sup> The resulting membrane was washed using a large amount of deionized water to remove unreacted PEG. It was then dried at  $40^\circ C$  in a vacuum oven. The resulting membrane was designated as the PANCMAN-g-PEG membrane. The grafting degree (DG) was calculated with the following equation:

$$DG (\%) = \frac{w_g - w_0}{w_0} \times 100$$

(19) Palit, S. R.; Ghosh, P. *J. Polym. Sci.* **1962**, *58*, 1225.

(20) Kang, I.-K.; Kwon, B. K.; Lee, J. H.; Lee, H. B. *Biomaterials* **1993**, *14*, 787.

(21) Oh, S. J.; Jung, J. C.; Zin, W. C. *J. Colloid Interface Sci.* **2001**, *238*, 43.

(22) Lin, Y. S.; Hlady, V.; Golander, C. G. *Colloids Surf., B* **1994**, *3*, 49.

(16) Ulbricht, M.; Matuschewski, H.; Oechel, A.; Hicke, H. G. *J. Membr. Sci.* **1999**, *115*, 31.

(17) Nie, F.-Q.; Xu, Z.-K.; Ming, Y.-Q.; Kou, R.-Q.; Liu, Z.-M.; Wang, S.-Y. *Desalination*, in press.

(18) Xu, Z.-K.; Kou, R.-Q.; Liu, Z.-M.; Nie, F.-Q.; Xu, Y.-Y. *Macromolecules* **2003**, *36*, 2441.

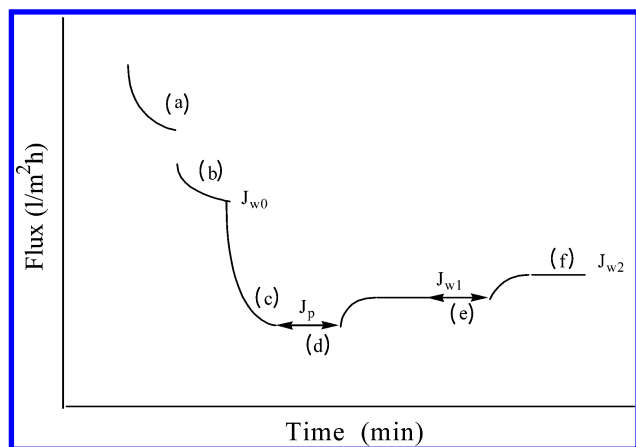


**Figure 2.** Filtration protocol: (a) compaction step; (b) deionized water filtration step; (c) BSA solution filtration step; (d) deionized water cleaning step; (e) chemical cleaning step; (f) deionized water cleaning step;  $J_{w0}$ , initial deionized water flux;  $J_p$ , 1 g/L BSA solution flux;  $J_{w1}$ , deionized flux after water cleaning;  $J_{w2}$ , deionized water flux after chemical cleaning.

where  $w_0$  and  $w_g$  are the weight of a membrane before and after the grafting reaction, respectively. The grafting degree was also calculated from the assumption that one anhydride group reacts with one PEG chain.

**Fourier Transform Infrared Spectroscopy.** To investigate the chemical changes between the unmodified and modified dense membranes and confirm the immobilization of PEG on the membrane surface, Fourier transform infrared spectroscopy (FT-IR, Vector 22) with an ATR unit (KRS-5 crystal, 45°) was used.

**Elemental Analysis (EA).** Elemental analysis was used to detect the atomic composition of the unmodified and modified porous membranes. The weight percent of carbon, hydrogen, and nitrogen of each sample was obtained from an elemental analyzer (EA1110, Carco Erba Co., Italy), and then that of oxygen was calculated from the EA data.

**Hydrophilicity Measurements.** The hydrophilicity of the membrane surface was characterized on the basis of pure water contact angle and adsorption measurements. Using a sessile drop method, water contact angle was measured at room temperature on a contact angle goniometer (KRÜSS DSA10-MK) equipped with video capture. A total of 50  $\mu$ L of deionized water was dropped onto a dry dense membrane with a microsyringe in an atmosphere of saturated water vapor. At least 10 contact angles were averaged to get a reliable value. Water adsorption was defined as  $(w_2 - w_1)/s$ , where  $w_1$  and  $w_2$  represent the weight of the dried membrane and the membrane soaked in water for 24 h at  $22 \pm 0.5$  °C, respectively, and  $s$  is the effective area of the tested membrane. The reported values were the mean of at least 10 experiments, and the standard deviation was within ca.  $\pm 5\%$ .

**Scanning Electron Microscopy.** The surface morphologies of the unmodified and modified membranes were examined by scanning electron microscopy (SEM) using a CAMBRIDGE S-260 scanning microscope. For this purpose, membrane samples were washed with a water–ethanol–hexane sequence, dried at room temperature, and then coated with a 20 nm gold layer before SEM analysis.

**Filtration Experiments.** The filtration protocol, which is shown in Figure 2, was similar to that of Pieracci et al.<sup>9,10</sup> Each membrane was first compacted for 30 min at 0.15 MPa. Then, the pressure was lowered to 0.10 MPa and the flux of deionized water ( $J_{w0}$ ) was measured by weighing permeate until consecutive recorded values differed by less than 2% ( $J_0$ ). Next, a 1 g/L BSA solution was added to the reservoir and the filtering experiment was performed at 0.10 MPa for 30 min; the permeate flux at the end of BSA solution filtration was denoted as  $J_p$ . After BSA solution filtration, the membrane was cleaned for 1 min three times to remove weakly attached BSA, and then the deionized water flux ( $J_{w1}$ ) was measured at 0.10 MPa. The membrane was filled with a 500 ppm NaOCl solution and filtered for 1 h at 0.10 MPa. Thereafter, the membrane was cleaned with deionized water, and the additional filtering of deionized water was

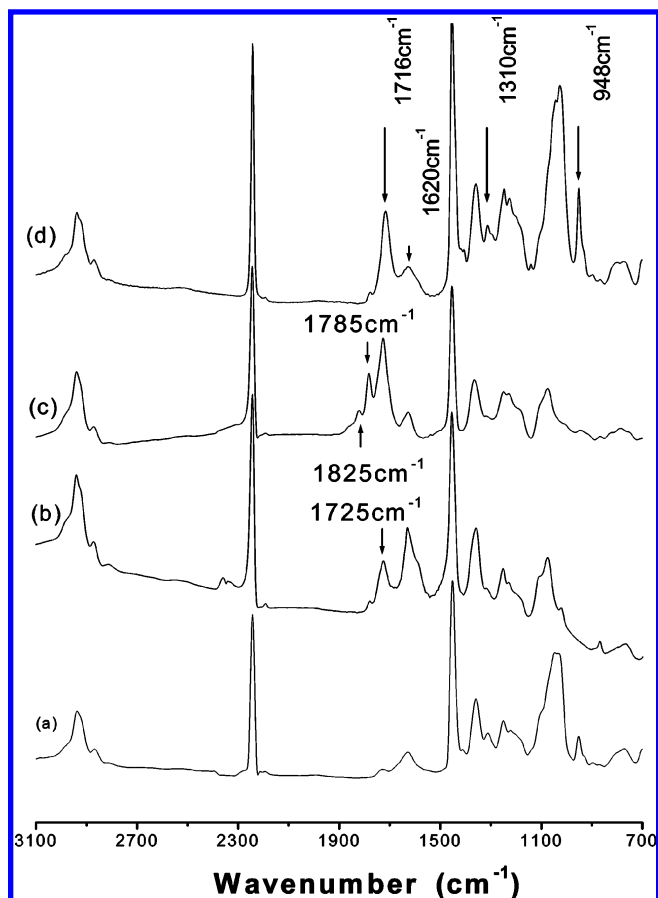


**Figure 3.** FT-IR/ATR spectra for the PAN-based dense membrane: (a) PAN; (b) PANCMA; (c) PANCMA<sub>n</sub>; (d) PANCMA<sub>n</sub>-g-PEG.

performed for 20 min in order to completely remove the remaining NaOCl. The next measured deionized water flux was  $J_{w2}$ . The reported data were the mean value of triplicate samples for each membrane.

The amount of adsorbed BSA that had not been removed after chemical cleaning was determined by measuring the weight of the membrane before and after the filtration experiment, which was completely dried and stored in a desiccator under nitrogen purge.

**Adhesion of Blood Platelets on the Membranes.** Fresh platelet-rich plasma (PRP), which was obtained from 20 mL of human fresh blood by centrifugation at 1000 rpm for 10 min, was used in all experiments. All samples of the dense flat membrane ( $1 \times 1$  cm<sup>2</sup>) were cut and placed in tissue culture plates, and 20  $\mu$ L of fresh PRP was dropped on the center of the tested membranes and incubated at  $22 \pm 0.5$  °C for 30 min. The tested membranes were rinsed gently with a phosphate buffered saline (PBS) solution, after which the adhered platelets were fixated with 2.5 wt % glutaraldehyde in PBS for 30 min. Finally, the samples were washed with PBS and dehydrated with a series of ethanol/water mixtures of increasing ethanol concentration (30, 40, 50, 60, 70, 80, 90, and 100% ethanol, 10 min in each mixture).<sup>23–24</sup> The samples were coated with gold and investigated by scanning electron microscopy (SEM). The status of adhered platelets on the membrane surface was examined from four different places on the same membranes at a 1000 magnification. All results were the average of four parallel experiments.

## Results and Discussion

Figure 3 shows the FT-IR/ATR spectra of the studied membranes. The spectrum of the PANCMA membrane

(23) Wetzels, G. M. R.; Koole, L. H. *Biomaterials* **1999**, *20*, 1879.

(24) Higuchi, A.; Shirano, K.; Harashimaa, M.; Yoon, B. O.; Haraa, M.; Hattori, M.; Imamura, K. *Biomaterials* **2002**, *23*, 2659.



**Table 1. Typical Characteristics of the PAN-Based Membranes**

sample no.	conversion of carboxyl <sup>a</sup> (%)	degree of grafting (%)	water adsorption ( $\times 10^{-3}$ g/cm <sup>2</sup> )	contact angle (deg)	porosity ratio, $P_r^b$ (%)
PAN			7.72	68.3 $\pm$ 0.2	83.7
PANcMA			12.05	48.2 $\pm$ 0.1	91.3
PANcMAN	58.6 $\pm$ 2.0		9.93	57.2 $\pm$ 0.1	81.1
PANcMAN- <i>g</i> -PEG		11.2 $\pm$ 0.3	20.38	31.4 $\pm$ 0.3	78.4

<sup>a</sup> The conversion ratio of carboxyl was determined by a modified rhodamine–carboxyl interaction method.<sup>19–20</sup> <sup>b</sup>  $P_r = (w_1 - w_2)/sld_{\text{water}} \times 100\%$ , where  $w_1$  and  $w_2$  represent the weights of the dried membrane and the membrane soaked in water for 24 h, and  $s$ ,  $l$ , and  $d$  represent the effective area, membrane thickness, and water density, respectively.

**Table 2. Elemental Analysis of the PAN-Based Membranes**

sample no.	nitrogen (wt %)	carbon (wt %)	hydrogen (wt %)	oxygen (wt %)
PANcMA	25.12	64.88	5.61	4.40
PANcMAN	25.38	65.56	5.49	3.47
PANcMAN- <i>g</i> -PEG	22.84	63.97	5.82	7.28

showed an absorbance band at 1725 cm<sup>-1</sup>, which was the characteristic band for carboxyl (Figure 3b). Converting carboxyl into anhydride could be confirmed by the appearance of two absorbance bands at 1785 and 1825 cm<sup>-1</sup> (Figure 3c). Using a modified rhodamine–carboxyl interaction method,<sup>19,20</sup> it was found that 58.6% of the carboxyl groups in the PANcMA membrane were converted into anhydride groups in the PANcMAN membrane (Table 1). This high conversion ratio might be ascribed to the reorganization of maleic acid groups in the surface region of the membranes. Due to the hydrophilic characteristics, maleic acid groups in the copolymer chains would reorientate and concentrate on membrane surfaces when phase separation took place in water. Compared with the spectrum of PANcMAN (Figure 3c), the characteristic bands of anhydride disappeared in the spectrum of PANcMA-*g*-PEG (Figure 3d), while the 1716 cm<sup>-1</sup> band for the C=O stretching vibration of the ester group appeared. Furthermore, the 1060 cm<sup>-1</sup> band for the C–O stretching vibration enhanced. On the other hand, the weight percentages of nitrogen, carbon, hydrogen, and oxygen for different membranes are summarized in Table 2. It was found that, with the conversion of carboxyl into anhydride, the weight percentages of hydrogen and oxygen decreased, while those of nitrogen and carbon increased. Nevertheless, the weight percentages of both oxygen and hydrogen had an obvious increase due to the reaction of PEG with the PANcMAN membrane. All these results indicated clearly that PEG was immobilized on the membrane surface by the esterification reaction.

The morphological changes of the studied membranes were observed by SEM. As shown in Figure 4, compared with that of the PANcMA membrane, the pore size of the PANcMAN membrane diminished slightly due to the dehydration of carboxyl groups. Grafting PEG chains on the PANcMAN membrane surface further reduced the pore size for the PANcMAN-*g*-PEG membrane. Porosity values listed in Table 1 showed a decrease sequence of PANcMA > PANcMAN > PANcMAN-*g*-PEG, which was consistent with the results of SEM.

Water contact angle and water adsorption had been commonly used to characterize the relative hydrophilicity or hydrophobicity of the membrane surface. The static contact angles of these four PAN-based membranes are summarized in Table 1. It can be seen that the PAN membrane showed a maximum value (68°). Due to the introduction of hydrophilic carboxyl or anhydride, the contact angle of PANcMA and PANcMAN membranes was lower than that of the PAN membrane. Comparing the PANcMAN with the PANcMA membrane, converting

carboxyl to anhydride increased the contact angle because the former group was more hydrophilic than the latter. Nevertheless, the contact angle of the PANcMAN-*g*-PEG membrane was 31° and lower than half of that of the PAN membrane. This meant that introducing PEG chains on the membrane surface could effectively hydrophilize the PAN-based membranes. Water adsorption had a similar trend as that for contact angle because the hydrophilic surface more easily absorbed water. As a result, the hydrophobicity of the PAN-based membranes decreased following the sequence PAN > PANcMAN > PANcMA > PANcMAN-*g*-PEG, as the contact angle of PANcMAN-*g*-PEG was the smallest as compared to those of the other membranes.

When materials contact with blood, proteins were first adsorbed instantaneously onto surfaces and deformed; then platelets were adsorbed, activated, and aggregated so that platelets played a major role in the thrombus formation. Therefore, a study on platelets' adhesion to evaluate the blood compatibility of materials was important. Figure 5 shows the situation of platelets adhering on PAN, PANcMAN, PANcMA, and PANcMAN-*g*-PEG membranes from PRP. It can be seen obviously that many platelets adhered on the PAN membrane surface, while PANcMA and PANcMAN membranes showed a slight suppression of platelets adhesion. On the other hand, platelets were rarely observed on the PANcMAN-*g*-PEG membrane. The density of adherent platelets was approximately 2476 per mm<sup>2</sup> for PAN, 1375 per mm<sup>2</sup>, for PANcMAN, 982 per mm<sup>2</sup> for PANcMA, and 294 per mm<sup>2</sup> for PANcMAN-*g*-PEG, respectively. It was also found that the amount of adsorbed BSA remaining on the membrane after chemical cleaning decreased significantly with an increase of the hydrophilicity. The value of PANcMAN-*g*-PEG was only 32.3% of that of PAN and 40.7% of that of PANcMAN. All these results indicated clearly that the biocompatibility of the PAN-based membranes was improved efficiently with the immobilization of PEG on the surface. From the literature,<sup>15,25–35</sup> PEG as a surface-

(25) Ko, Y. G.; Kim, Y. H.; Park, K. D.; Lee, H. J.; Lee, W. K.; Park, H. D.; Kim, S. H.; Lee, S.; Ahn, D. G. *Biomaterials* **2001**, *22*, 2115.

(26) McPherson, T.; Kidane, A.; Szleifer, I.; Park, K. *Langmuir* **1998**, *14*, 176.

(27) Efremova, N. V.; Sheth, S. R.; Leckband, D. E. *Langmuir* **2001**, *17*, 7628.

(28) Harris, J. M., Ed. *Poly(ethylene glycol) Chemistry – Biotechnical and Biomedical Applications*; Plenum Press: New York, 1992.

(29) Sofia, S. J.; Premnath, V.; Merrill, E. W. *Macromolecules* **1998**, *31*, 5059.

(30) Malmsten, M.; Emoto, K.; Van Alstine, J. *J. Colloid Interface Sci.* **1998**, *202*, 507.

(31) Kingshott, P.; Thissen, H.; Griesser, H. J. *Biomaterials* **2002**, *23*, 2043.

(32) Kingshott, P.; Griesser, H. J. *Curr. Opin. Solid State Mater. Sci.* **1999**, *4* (4), 403.

(33) Huang, N.-P.; Michel, R.; Voros, J.; Textor, M.; Hofer, R.; Rossi, A.; Elbert, D. L.; Hubbell, J. A.; Spencer, N. D. *Langmuir* **2001**, *17*, 489.

(34) Kenausis, G. L.; Voros, J.; Elbert, D. L.; Huang, N.; Hofer, R.; Ruiz-Taylor, L.; Textor, M.; Hubbell, J. A.; Spencer, N. D. *J. Phys. Chem. B* **2000**, *104*, 3298.

(35) Vert, M.; Domurado, D. *J. Biomater. Sci. Polym. Ed.* **2000**, *11*, 1307.

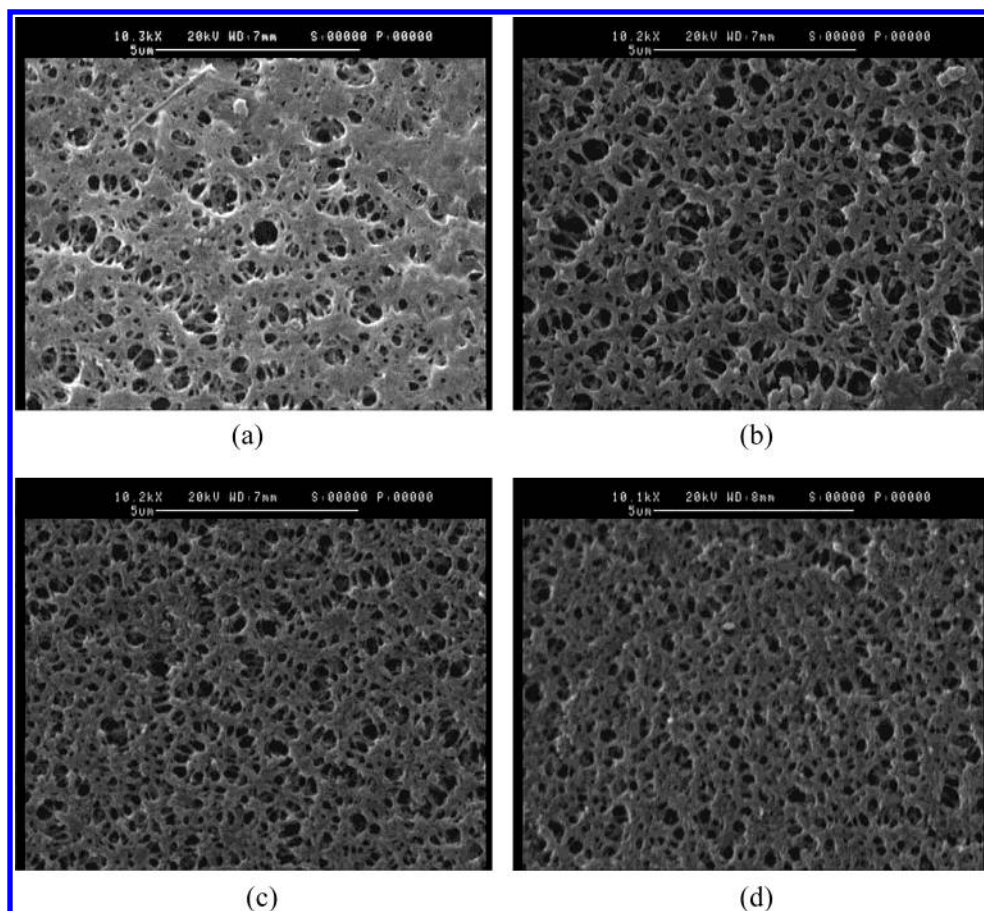


**Figure 4.** SEM photographs of the PAN-based membrane surfaces: (a) PAN; (b) PANCMA; (c) PANCMA<sub>n</sub>; (d) PANCMA<sub>n</sub>-*g*-PEG.

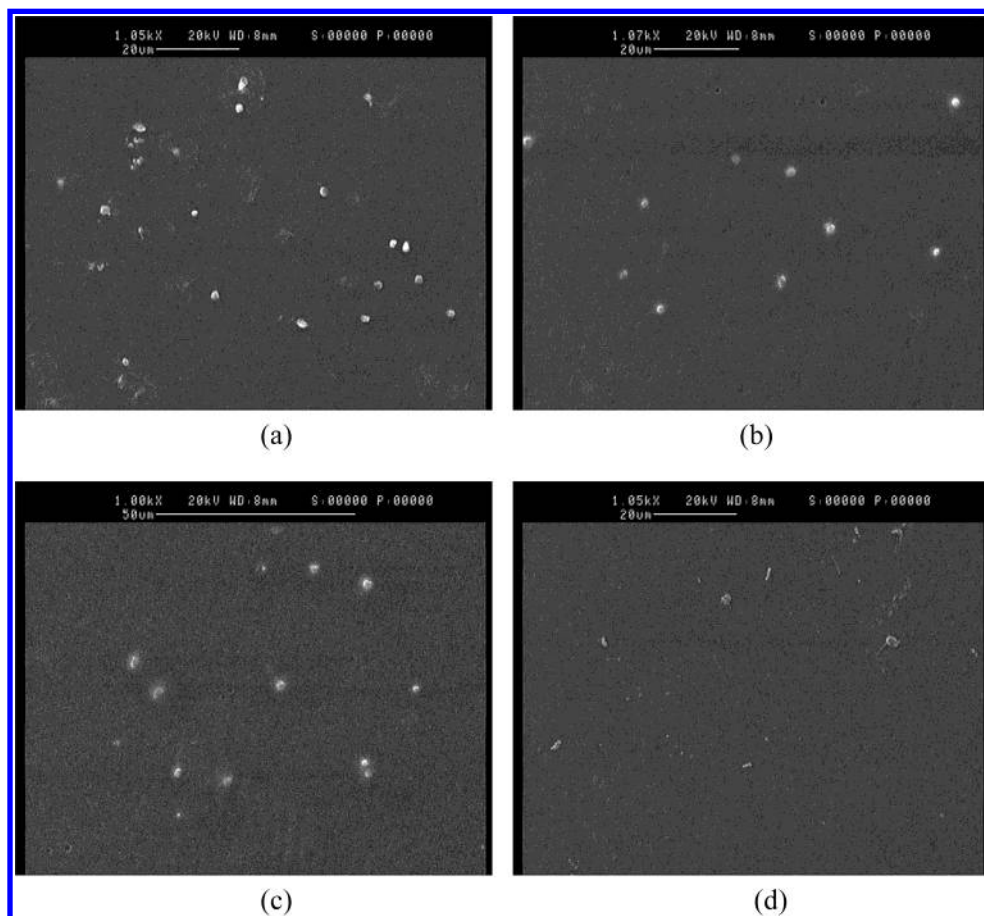


**Figure 5.** Adhesion of platelets on the dense membrane surface: (a) PAN; (b) PANCMA; (c) PANCMA<sub>n</sub>; (d) PANCMA<sub>n</sub>-*g*-PEG.



**Table 3. Filtration Performances of the PAN-Based Membranes<sup>a</sup>**

sample	$J_{w0}$ (L/(m <sup>2</sup> h))	$J_p$ (L/(m <sup>2</sup> h))	$J_{w1}$ (L/(m <sup>2</sup> h))	$J_{w2}$ (L/(m <sup>2</sup> h))	BSA adsorption <sup>b</sup> (μg/mg)
PAN	372	104	138	190	14.26
PANCMAN	450	233	289	342	7.97
PANCMAN	389	164	227	269	11.32
PANCMAN- <i>g</i> -PEG	871	644	707	782	4.61

<sup>a</sup> The filtration test was conducted at a constant transmembrane pressure of 0.1 MPa and a system temperature of  $22 \pm 0.2$  °C. Error range:  $\pm 5\%$ . <sup>b</sup> The amount of BSA adsorbed onto the membrane after chemical cleaning.

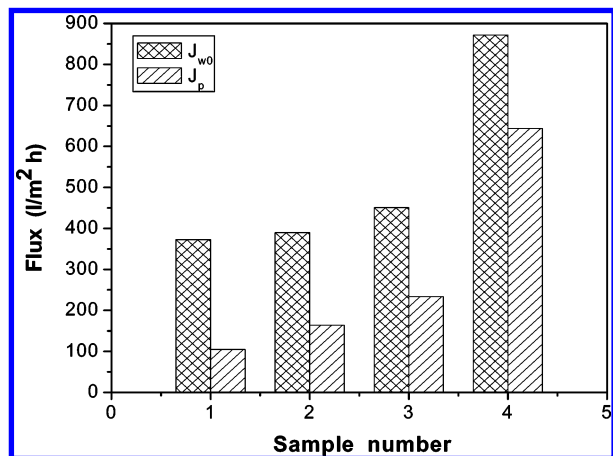


**Figure 6.** Permeation fluxes of deionized water and BSA solution through the PAN-based membranes: (1) PAN; (2) PANCMAN; (3) PANCMAN; (4) PANCMAN-*g*-PEG.

modifying agent is clearly the most effective molecule at reducing bioadhesion (protein adsorption, platelet deposition, and cell adhesion). The best reports have shown that protein adsorption can be suppressed to a fraction of the uncoated surface or even remain undetected when analyzed by the most sensitive analytical methods.<sup>29–32</sup> The majority of the models of grafted PEG attribute its protein resistance to two main ingredients, namely, (i) the steric or osmotic repulsion between proteins and the chains and (ii) the assumption that the  $-\text{CH}_2\text{CH}_2\text{O}-$  segments completely repel protein.<sup>28</sup> Results obtained in this work were consistent with the wide acceptance of this view.

To investigate the performance of the studied membranes, deionized water and BSA solution filtration experiments were carried out. Typical results for the permeation fluxes of deionized water and BSA solution through the PAN-based membranes are depicted in Table 3 and Figure 6. The symbols  $J_{w0}$  and  $J_p$  were defined as the flux of deionized water and BSA solution, respectively. As shown in Figure 6, both  $J_{w0}$  and  $J_p$  increased in the order PAN < PANCMAN < PANCMAN < PANCMAN-*g*-PEG. This agreed with the sequence of the hydrophilicity increase for the membranes mentioned above. The PANCMAN membrane had a lower permeation flux than that of the PANCMAN membrane because the latter had a better hydrophilicity and larger pore size than those of the former, as mentioned above. It seems that the hydrophilicity of the membrane surface impacted the permeation flux more effectively than the pore size. A similar phenomenon was observed in our previous work about the surface modification of a microporous polypropylene membrane by graft polymerization.<sup>36</sup> Therefore, although the pores were slightly narrowed from PANCMAN to PANCMAN-*g*-PEG, however, the BSA solution flux increased from 233 L/(m<sup>2</sup> h) for PANCMAN to 644 L/(m<sup>2</sup> h) for PANCMAN-*g*-PEG. Compared with the PAN membrane, PANCMAN-*g*-PEG showed a 6-fold increase

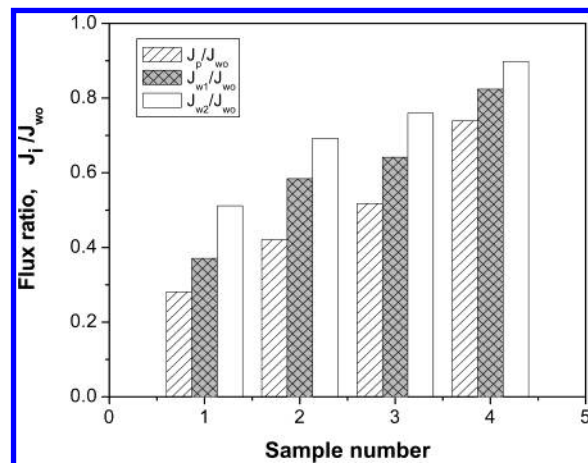


**Figure 7.** Effects of deionized water cleaning and chemical cleaning on the flux ratios of PAN-based membrane filtration performances: (1) PAN; (2) PANCMAN; (3) PANCMAN; (4) PANCMAN-*g*-PEG.

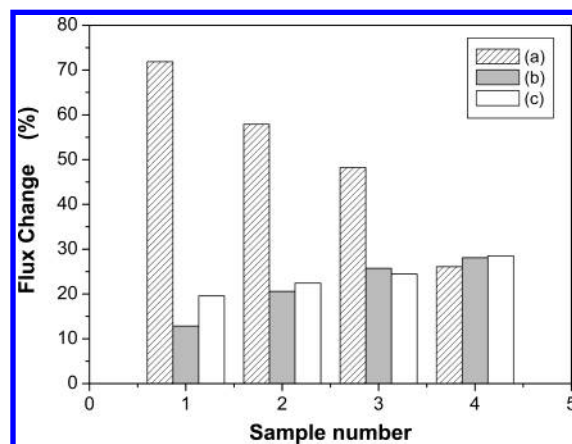


**Figure 8.** Flux changes of PAN-based membranes during filtration and after water and chemical cleaning: (1) PAN; (2) PANCMAN; (3) PANCMAN; (4) PANCMAN-*g*-PEG.

in BSA solution flux. This was reasonable because the hydrophobic interaction was weakened between BSA molecules and the hydrophilized membrane surface and, in turn, membrane fouling caused by BSA adsorption was reduced. The BSA adsorption data listed in Table 3 on the membrane surface supported this explanation.

The effect of water cleaning and chemical cleaning on membrane filtration performance is shown in Figure 7. In this figure, the relative ratios of BSA solution permeation flux ( $J_p$ ), water permeation flux after water cleaning ( $J_{w1}$ ), and water permeation flux after chemical cleaning ( $J_{w2}$ ) to water permeation flux ( $J_{w0}$ ) are presented. It was found that  $J_p/J_{w0}$ ,  $J_{w1}/J_{w0}$ , and  $J_{w2}/J_{w0}$  increased according to the hydrophilicity of the studied membranes. The flux recovered by water and chemical cleaning was greatly improved with the immobilization of hydrophilic PEG chains on the membrane surface.  $J_{w2}/J_{w0}$  of PANCMAN-*g*-PEG reached 0.90; this indicated that the flux recovered

(36) Kou, R.-Q.; Xu, Z.-K.; Deng, H.-T.; Liu, Z.-M.; Seta, P. *Langmuir* **2003**, *19*, 6869.

by chemical cleaning almost reached its initial water permeation flux.

Figure 8 shows the percent of total fouling  $((1 - J_p/J_{w0}) \times 100)$ , the flux recovery by water cleaning  $((J_{w1} - J_p)/(J_{w0} - J_p) \times 100)$ , and the flux recovery by chemical cleaning  $((J_{w2} - J_{w1})/(J_{w0} - J_p) \times 100)$ .<sup>9,10</sup> It can be seen that the total fouling decreased from 71.86% for PAN to 48.22% for PANCMA to 26.08% for PANCMA-*g*-PEG. All these results proved that the antifouling property was effectively improved by the immobilization of hydrophilic PEG on the membrane surface. Furthermore, with an increase of the hydrophilicity, both  $((J_{w1} - J_p)/(J_{w0} - J_p) \times 100)$  and  $((J_{w2} - J_{w1})/(J_{w0} - J_p) \times 100)$  increased, which revealed that when the adsorption of proteins took place on the membrane surface, the proteins on the hydrophilic membrane surface were removed more easily by deionized water and chemical cleaning.

### Conclusions

Through the esterification reaction of anhydride groups on PANCMA membrane surfaces with the hydroxyl groups in PEG, PEG could be immobilized on a membrane surface to effectively improve the biocompatibility and antifouling property of a PAN-based membrane. Hydrophilicity on the basis of water contact angle and adsorption measurements for the membranes enhanced in a PAN < PANCMA < PANCMA-*g*-PEG sequence. The density of adherent platelets on the membrane surface

decreased following the same sequence as that for the hydrophilicity increase. The amount of adsorbed BSA on the PANCMA-*g*-PEG membrane was reduced to about 67.65% of that on the PAN membrane because the hydrophobic interactions between BSA molecules and the membrane surface were prevented by grafted PEG chains. The PANCMA-*g*-PEG membrane showed the best biocompatibility among the studied membranes. Although the pore size and porosity of the PANCMA-*g*-PEG membrane decreased due to the grafting of PEG, the permeation fluxes of water and BSA solution increased due to the increased membrane hydrophilicity and the decreased BSA adsorption on the membrane surface. Moreover, the total fouling decreased from 71.86% for PAN to 48.22% for PANCMA to 26.08% for PANCMA-*g*-PEG. The flux recovery of the modified membrane after water and chemical cleaning was superior to that of unmodified membranes. Further works concerning the influences of the immobilization density and the molecular weight of the PEG on PANCMA-*g*-PEG membrane performance will be described in a forthcoming paper.

**Acknowledgment.** The financial support from the National Nature Science Foundation of China (Grant No. 50273032) and the High-Tech Research and Development Program of China (Grant No. 2002AA601230) is gratefully acknowledged.

LA035315H